Low Cost Corrosion Damage Mitigation and Improved Fatigue Performance of Low Plasticity Burnished 7075-T6

Paul S. Prevéy and John Cammett

(Submitted 17 October 2000; in revised form 5 April 2001)

Low plasticity burnishing (LPB) has been investigated as a surface enhancement process and corrosion mitigation method for aging aircraft structural applications. Compressive residual stresses reaching the alloy yield strength and extending to a depth of 1.25 mm (0.050 in.) deeper than typical corrosion damage is achievable. Excellent surface finish can be achieved with no detectable metallurgical damage to surface and subsurface material. Salt fog exposures of 100 and 500 h reduced the fatigue strength at 2×10^6 cycles by 50%. The LPB of the corroded surface, without removal of the corrosion product or pitted material, restored the 2×10^6 fatigue strength to greater than that of the original machined surface. The fatigue strength of the corroded material in the finite life regime (10^4 to 10^6 cycles) after LPB was 140 MPa (20 ksi) higher than the original uncorroded alloy and increased the life by an order of magnitude. Ease of adaptation to computer numerical control (CNC) machine tools allows LPB processing at costs and speeds comparable to machining operations. Low plasticity burnishing offers a promising new technology for mitigation of corrosion damage and improved fatigue life of aircraft structural components with significant cost and time savings over current practices.

Keywords 7075-T6 aluminum, corrosion mitigation method, low plasticity burnishing, residual stresses

Introduction

High cycle fatigue (HCF) damage, often initiated from corrosion pitting, is a growing threat to safety and performance of naval aircraft. Maintenance requirements to inspect for fatigue damage, replace parts, and rework to remove corrosion damage increase the cost of operation. The down time required to perform inspections and repairs, during which aircraft are not available for combat, significantly impacts military readiness. Estimated annual costs for corrosion inspection and repair of naval aircraft alone exceed $1 billion. Currently, more than 30% of military aircraft are over 20 years old and over 90% are expected to exceed a 20 year life by the year 2015.[1]

Corrosion pits are a common site of fatigue crack initiation in the aluminum alloy structural components of naval aircraft. Corrosion pitting results in intergranular corrosion to a depth, depending upon the time of exposure, temperature, and the service environment of the aircraft. The pronounced fatigue strength reduction caused by salt pit corrosion is well established for both steels[2] and aluminum alloys[3] and results typically in the reduction of the endurance limit to nominally half of the uncorroded value. Common overhaul practice requires hand rework or machining to remove the pitted layer followed by shot peening as a surface enhancement technique to improve fatigue life, a time consuming and costly practice.

Paul S. Prevéy, Lambda Research, Cincinnati, OH; and **John Cammett,** Naval Aviation Depot, MCAS Cherry Point, NC. Contact e-mail: kbellamy@lambda-research.com.

New surface enhancement technologies have been developed that can provide a layer of compressive residual stress of sufficient depth to effectively eliminate the influence of the salt pit corrosion. Laser shock peening (LSP)[4,5] has been demonstrated to produce a pronounced increase in fatigue life of samples containing deep foreign object damage. Unfortunately, laser shocking is extremely expensive to perform, and slow and difficult to incorporate into aircraft manufacturing and overhaul shop environments. More recently, low plasticity burnishing (LPB)[6] has been demonstrated to provide comparable depth and magnitude of compressive residual stress at far lower cost than for LSP. The LPB process can be performed on conventional CNC machine tools at costs and speeds comparable to conventional machining operations, such as surface milling. The residual stress distributions developed in IN718[6] and in Ti-6Al-4V[7] produced by LPB have exceeded 1 mm in depth, well beyond the depth of typical corrosion pits that serve as the initiation sites for fatigue cracks.

Recent work in modeling[8] of corrosion pit crack growth in 7075-T6 has indicated that the pits can be treated as semi-elliptical cracks having depths on the order of average pit depth for the purpose of predicting the degradation of fatigue strength caused by corrosion. Therefore, if a layer of compressive residual stress of sufficient magnitude and depth can be induced into the surface of the part, to a depth greater than the existing pits or microcracks, the growth of fatigue cracks might be arrested.

The purpose of this study was to investigate the effectiveness of LPB in creating a layer of compressive residual stress in 7075-T6 aluminum. The effect of the compressive layer on the fatigue strength of salt fog-corroded 7075-T6 machined surfaces was used to test performance.

Table 1 7075-T6 $^1/_2$ in. plate composition

Element	Plate analysis (wt.%)	AMS 4045 limits
Zn	5.5	5.1–6.1
Mg	2.44	2.1–2.9
Cu	1.45	1.2–2.0
Fe	0.25	0.7 max
Cr	0.19	0.18–0.40
Si	0.07	0.50 max
Ti	…	0.20 max
Mn	…	0.30 max
Al	Remainder	Remainder

Experimental Technique

Material

Aluminum alloy 7075-T6 was acquired in the form of 12.5 mm (0.5 in.) plate to AMS 4045. In the -T6 heat treated condition, the material was found to have a hardness of 89 HRB (Hardness Rockwell B) and electrical conductivity of 33% International Annealed Copper Standard (IACS). Chemistry was verified to be within limits of the AMS 4045 specification, as shown in Table 1.

Tensile properties were verified as 601 MPa (87.3 ksi) ultimate tensile strength, 0.2% yield strength of 542 MPa (78.7 ksi), and elongation of 11%.

Low Plasticity Burnishing

All currently available methods of surface enhancement develop a layer of compressive residual stress following mechanical deformation. The methods differ primarily in how the surface is deformed and in the magnitude and form of the resulting residual stress and cold work (plastic deformation) distributions developed in the surface layers.

Conventional air-blast shot peening is routinely applied to a wide variety of aircraft components. High velocity impact of each particle of shot produces a dimple with a region of compression in the center. Typical compressive residual stress distributions reach a maximum approaching the alloy yield strength and extend to a depth of 0.05 to 0.5 mm (0.002 to 0.020 in.) The magnitude of compression achieved depends primarily upon the mechanical properties of the alloy. The depth of the compressive layer and the degree of cold working depend upon the peening parameters, including shot size, velocity, coverage, and impingement angle. Because each shot impacts the surface at a random location, peening for sufficient time to achieve uniform surface coverage results in many multiple impacts producing a highly cold-worked surface layer.[9]

Conventional shot peening produces from 10 to 50% cold work, much more than from grinding, machining, or other common surface finishing processes.[10] Cold work is cumulative, and repeated applications of shot peening can produce even more than 50% cold work. Both the depth and degree of cold working increase with peening intensity, with the most severe cold working at the surface. Surface compression often decreases during shot peening of work hardening materials as the yield strength of the surface increases with continued cold working.

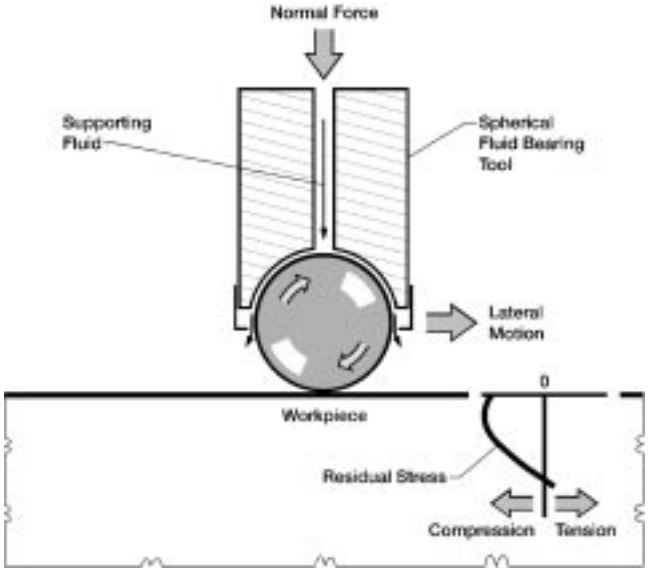

Fig. 1 LPB schematic

The concept of LPB originated as a means of producing a layer of compressive residual stress of high magnitude and depth with minimal cold work.[11] The process is characterized by a single pass of a smooth free-rolling spherical ball under a normal force sufficient to plastically deform the surface of the material, thereby creating a compressive layer of residual stress. The process is shown schematically in Fig. 1. The ball is supported in a fluid bearing with sufficient pressure to lift the ball off the surface of the retaining spherical socket. The ball is in mechanical contact only with the surface to be burnished and is free to roll on the surface of the work piece.

Although the tool designs and hydraulic systems differ, the LPB tooling is similar to "deep rolling" tools using a hydrostatically supported burnishing ball.[12,13,14] The LPB and deep rolling processes differ in the method of use and the level of cold work generated in developing the compressive layer. X-ray diffraction peak broadening and microhardness distributions generated by shot peening and deep rolling reveal that deep rolling produces cold work greater than shot peening. In contrast, LPB typically produces cold work an order of magnitude lower than shot peening.

Using CNC positioning, the tool path is controlled so that the surface is covered with a series of passes at a separation maintained to achieve maximum compression with minimum cold working. The tool may be moved in any direction along the surface of a complex work piece, as in a typical multiaxis CNC machining operation.

The burnishing ball develops subsurface Hertzian contact stresses in the work piece. These stresses act parallel to the plane of the surface and reach a maximum beneath the surface. With sufficient pressure applied normal to the surface, the subsurface stress exceeds the yield strength of the work piece material, thereby producing deep subsurface compression. The normal force required and the depth at which yielding first occurs depend upon the ball diameter.

The speed of burnishing, up to 500 sfm, has been found to have no effect upon the residual stress distribution produced.

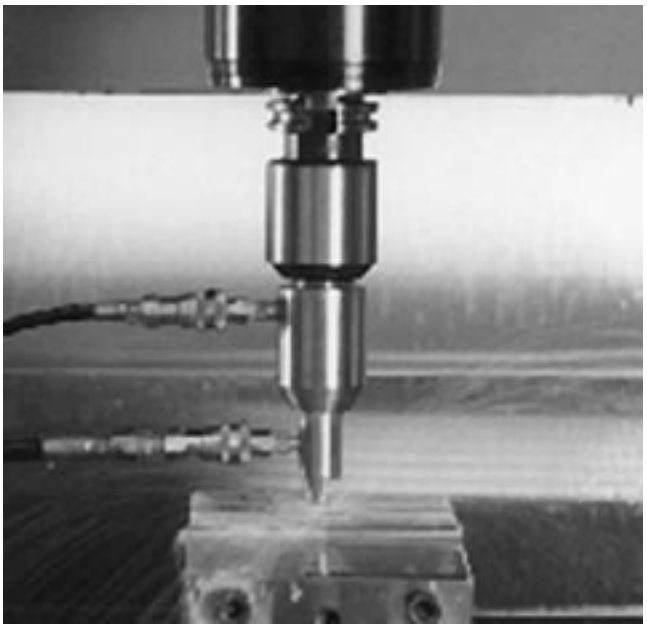

Fig. 2 LPB tool positioned for burnishing a coupon in a 20 HP vertical CNC mill

This allows application of the process at the highest practical CNC machining speeds.

The surface residual stress depends upon the normal force, feed, and mechanical properties of both the ball and work piece. Lateral plastic deformation of the surface is necessary to achieve surface compression. Processing parameters have been established empirically. With a poor choice of processing parameters, the surface can be left nearly stress free or even in tension. Empirical optimization has been used successfully to select parameters that leave the surface in compression.

The LPB tool designed to fit a CAT-40 tool holder in a Haas HP vertical CNC mill (Haas Automation, Inc., Oxnard, CA) is shown in Fig. 2. The quill of the machine is not rotated. The swivel links in the hydraulic hose allow exchange of the tool to and from the tool holder so that LPB processing can be incorporated into standard machining sequences in existing CNC machine tools. Injection of the fluid through the quill of the mill is also possible in a suitably equipped machine. With minor modification, the apparatus can be adapted to most horizontal and multiaxis mills, or lathes.

The control apparatus for the hydraulic system provides a constant flow of fluid to support the burnishing ball and a computer controlled feedback system to maintain the desired normal force and fluid pressure. The burnishing force and tool feed can be varied in order to "feather" the residual stress field, thereby providing a smooth transition at the perimeter of the burnished zone or to produce a distribution of residual stress appropriate for a specific application or applied stress field.

The burnishing ball is the only wear-prone component of the LPB tooling. High chromium steel, beta-silicon nitride, and sintered tungsten carbide balls, readily available from ball bearing applications, have been used successfully in the current apparatus. The surface finish achievable depends upon the finish of the ball. Bearing balls are commonly available with finishes of grade 25 (25 μin.) or better at costs less than cutting tool inserts.

X-ray Diffraction Characterization

Diffraction peak broadening, measured along with the residual stress, allows the amount of damage developed by surface enhancement methods to be accurately assessed. The method of quantifying the degree of cold working of metals, by relating the x-ray diffraction peak broadening to the equivalent true plastic strain, has been described previously.[10] The distribution of cold work as a function of depth into the deformed surface can be expressed in terms of the equivalent true plastic strain. If the degree of cold work is taken to be the equivalent amount of true plastic strain, the degree of cold work is then cumulative and is independent of the mode of deformation. Thus, the subsurface yield strength distribution can then be estimated from true stress-strain curves.[10] The macroscopic residual stress, of primary interest in design and life prediction, is determined in the conventional manner from the shift in the diffraction peak position.[15,16,17]

HCF Testing

Four-point bending was the HCF testing mode selected to provide maximum sensitivity to the surface condition.[18] Fatigue testing was conducted at room temperature on a Sonntag SF-1U fatigue machine (Baldwin Lima Hamilton, Philadelphia, PA) under constant sinusoidal load amplitude at 30 Hz, $R = 0.1$.

A bending fatigue specimen having a trapezoidal cross section was designed especially for the testing of highly compressive surface conditions created by surface enhancement methods. The test specimen provides a nominally 12.5 mm (0.5 in.) wide by 25 mm (1 in.) long region under uniform applied stress to minimize scatter in fatigue testing. The original gage section thickness of nominally 9 mm (0.375 in.) was chosen to be adequate to support the tensile stresses induced in the back of the specimen when a deep highly compressive layer was formed on the test surface. The gage section thickness was then reduced to 6 mm (0.25 in.) by milling the backside to ensure failure out of the highly compressive surface in four-point bending. The HCF samples were finished machined by milling using conventional end milling to simulate the surface conditions including residual stress and cold work that would be present on a machined structural aircraft component manufactured from 7075-T6.

Baseline S/N (stress/cyclic life) curves were developed for the as-machined condition and the machined condition plus LPB processing. The S/N curves were then developed for specimens that had been machined and then exposed to either 100 or 500 h in the salt fog environment. Half of the specimens given the 100 and 500 h exposures were then LPB processed. The S/N curves were then generated for the as-corroded and corroded plus LPB specimen groups.

Salt Fog Corrosion Exposure

The salt fog corrosion exposure was performed at 35 °C per ASTM B117, Standard Practice for Operating Salt Spray (Fog) Apparatus. The fog produced was such that 1 to 2 mL/h of 5 ± 1 mass% NaCl aqueous solution collected on each 80 cm^2

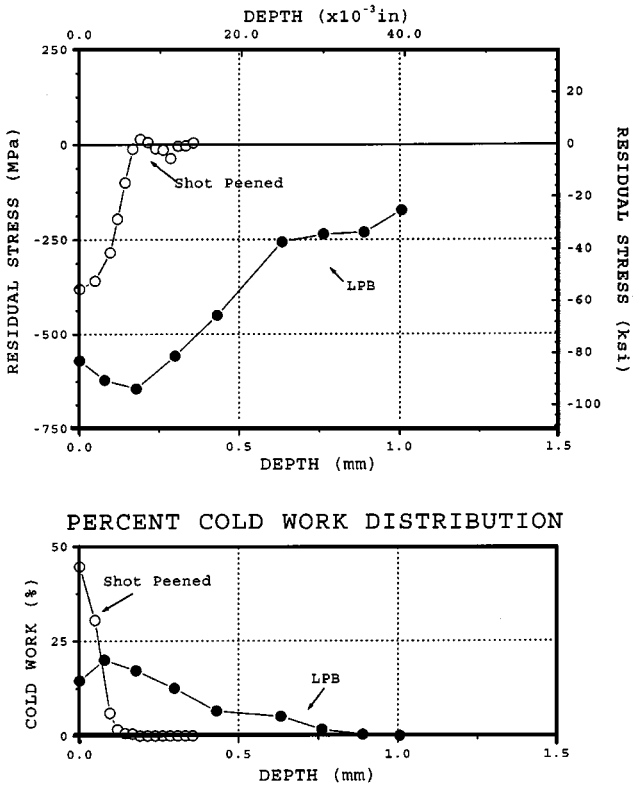

Fig. 3 Comparison of residual stress and half-width distribution in shot peened and LPB processed 7075-T6 aluminum

horizontal surface. The pH of the solution was maintained between 6.5 and 7.2. The salt fog exposure was performed at the Naval Air Depot at Cherry Point using a model TTC600 chamber manufactured by Q-Fog Corporation (Cleveland, OH).

The specimens were exposed in two groups with the test surface horizontal for 100 and 500 h. Following exposure to the salt fog, the samples were soaked and then rinsed in tap water, followed with a distilled water rinse to remove any salt solution remaining, and then dried. Patches of gray and white corrosion product evident on the surface of the samples were identified by x-ray diffraction as α-Al_2O_3. The corrosion product was not removed prior to testing or LPB processing.

Results and Discussion

Residual Stress Distributions

The residual stress distributions developed by the LPB parameters used in this investigation are shown in comparison to conventional shot peening in Fig. 3. Shot peening to an 8A intensity with CW14 shot for 200% coverage, a typical practice, produces compression to depths on the order of 0.2 mm (0.008 in.) reaching a maximum on the surface of nominally 350 MPa (50 ksi). The repeated impacts of the shot necessary to achieve coverage resulted in approximately 45% cold work at the shot-peened surface. In contrast, the LPB parameters used in this investigation produced maximum compression below the surface on the order of −650 MPa (−94 ksi). Maximum cold work of nominally 20% occurs below the surface and the compressive layer extends more than 1 mm (0.040 in.) into the surface. The LPB produced both a higher magnitude of compression and a greater depth than shot peening, well beyond the depth of corrosion pitting.

Table 2 Surface finish 7075-T6 aluminum effect of LPB after salt fog exposure

Salt fog exposure time (h)	Roughness (μin., Ra)	
	Machined	LPB
0	39 ± 7	8 ± 3
100	139 ± 34	31 ± 33
500	162 ± 36	68 ± 54

No attempt was made to optimize the LPB parameters used in this investigation other than to produce a deep layer of compression. Previous experience with LPB of IN718, Ti-6Al-4V, and 4340 steel indicates that, with proper selection of burnishing parameters, the amount of cold working could be reduced while maintaining comparable depth of compression. These parameters including normal force, ball size, ball material, and feed could be easily adjusted if further reduction of cold working is found to improve resistance to corrosion.

The effects of LPB processing on the surface finish of the original machined material and after 100 and 500 h exposure to salt fog are shown in Table 2. These are the results of three repeat measurements made on each of two samples representing the conditions shown. The effect on the original machined surface was to reduce the surface roughness from nominally 40 to 8 μin, Ra. Salt fog exposure produced a very rough and nonuniform surface finish resulting in a wide spread in roughness in the corroded condition, as indicated by the high standard deviations for the corroded specimens. For either 100 or 500 h exposure, the LPB reduced the surface roughness by nominally 100 μin, Ra.

Corrosion Damage

Fractographic examination of the fatigue failures and macroscopic examination of the exposed surfaces revealed that salt fog exposure resulted in uniform corrosion of the test surfaces. Pit depths averaged 0.10 to 0.13 mm (0.004 to 0.005 in.) with some pits extending to 0.25 mm (0.01 in.). After penetration of the surface, the corrosion crevices often were observed to progress laterally, thereby delaminating layers of material apparently following the elongated grain boundaries produced by rolling of the plate. Although no significant difference was observed in the type or depth of corrosion pits produced by the 100 and 500 h exposure, a greater density of pitting was evident for the 500 h exposures.

A typical macroscopic view of a corroded specimen surface after 100 h exposure is shown in Fig. 4. The macroscopic view of a typical corrosion pit crack nucleation site on a machined +100 h salt fog exposed specimen is shown in Fig. 5(a). The same corrosion pit nucleation site is shown in the scanning electron microcopy (SEM) micrograph in Fig. 5(b).

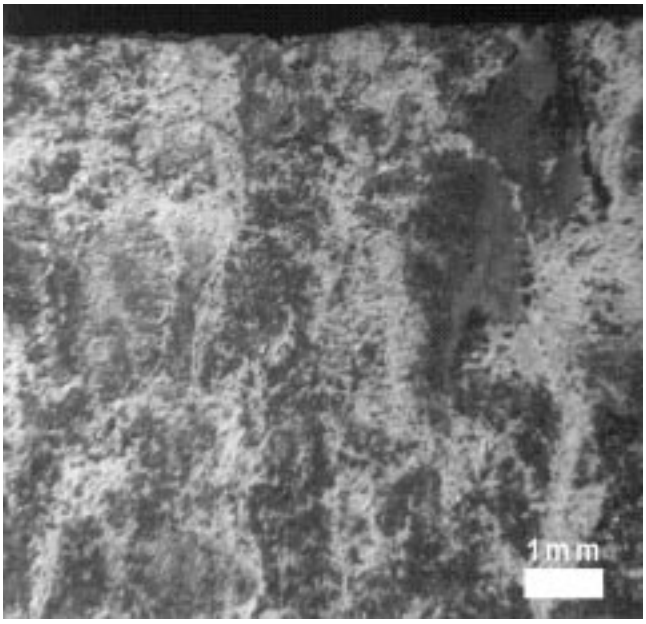

Fig. 4 Macroscopic appearance of a specimen after 100 h exposure showing patches of Al_2O_3 corrosion product

HCF Performance

The S/N curves generated for the as-machined, machined + LPB, corroded, and corroded + LPB specimens are summarized in Fig. 6. Fatigue tests were terminated after nominally 2×10^6 with a few exceptions running out to as much as 10^7 cycles. Most of the conditions for which the samples were tested appeared to exhibit an endurance limit, implying infinite life below some threshold stress level. Because of the limited testing time and small number of tests performed, however, this cannot be confirmed, especially for the longer running tests after LPB processing. Therefore, the results are considered and compared in terms of the fatigue life at nominally 2×10^6 cycles. The data are presented as semilogarithmic S/N curves at $R = 0.1$ in terms of the maximum stress.

The machined (end milled) surface condition produced an apparent endurance limit behavior and a fatigue strength at nominally 2×10^6 cycles on the order of 200 MPa (30 ksi). Salt fog exposure for either 100 or 500 h reduced the fatigue strength in the finite life range, from 10^4 to 2×10^5 cycles, slightly, perhaps on the order of 35 MPa (5 ksi), but reduced the fatigue strength at 2×10^6 to nominally half that of the original machined surface before corrosion. Loss of nominally half the extended life fatigue strength following salt fog corrosion appears to be typical of the degradation reported in the literature.[3]

The LPB of the machined surface without corrosion exposure produced the highest fatigue strength at any life. Burnishing directly over the corroded surface produced by either 100 or 500 h salt fog exposure resulted in nearly identical improved fatigue performance, even exceeding that of the original machined surface. The LPB appears to have at least fully restored the extended life fatigue strength at 2×10^6 to that of the original as-machined surface. Several data points indicate improved long-term fatigue strength by as much as nominally 35 MPa (5 ksi) at lives exceeding 2×10^6. In the finite life regime between 10^4 and 10^6 cycles, LPB processing of either the original machined or the machined +100 or 500 h salt fog corrosion has increased the life at a given stress level by a factor of 10. Considered in terms of the increased fatigue strength at a fixed life, the fatigue strength at 10^5 cycles after LPB processing of the machined or corroded surfaces improved by nominally 170 MPa (25 ksi), a pronounced effect on a material having HCF strength on the order of 205 MPa (30 ksi).

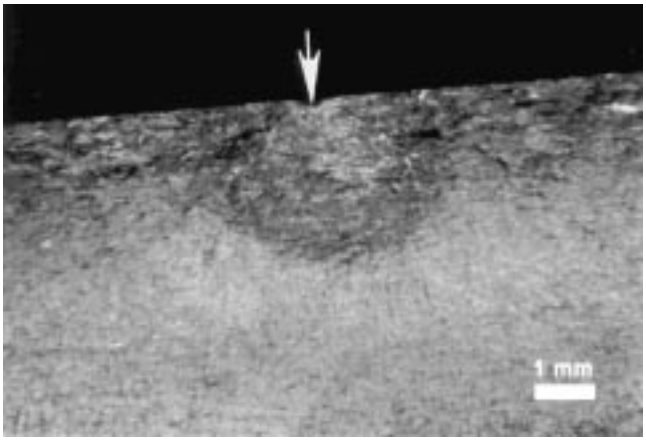

(**a**)

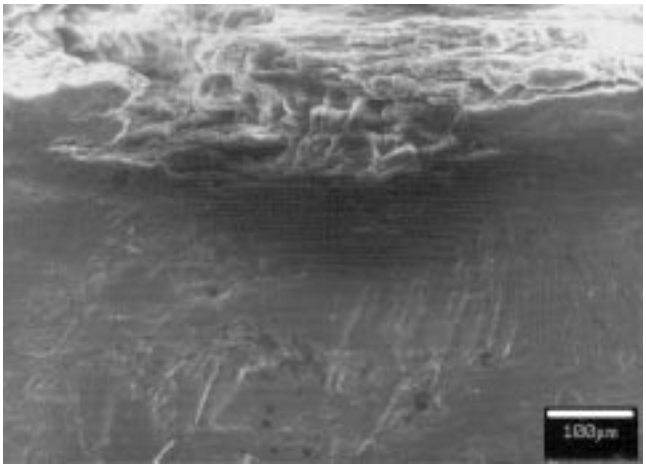

(**b**)

Fig. 5 (**a**) Arrow indicates macroscopic appearance of fatigue origin at the site of corrosion after 100 h salt fog exposure. (**b**) Microscopic appearance of the fatigue origin at the site of corrosion pit shown in (a) after 100 h salt for exposure

Fractography

Fatigue failures occurred in the as-machined specimens exclusively from the end milled-end cut machined surfaces. Generally, single fatigue origins occurred in specimens tested at lower stresses with a normal tendency toward multiple origins in specimens tested at higher stress levels. Specimens that were machined and then subjected to 100 or 500 h salt fog exposures suffered pitting, which degraded fatigue strength relative to the as-machined condition. The fatigue strength degradation was the same for both exposure times despite a greater population of pits in the 500 h exposed specimens.

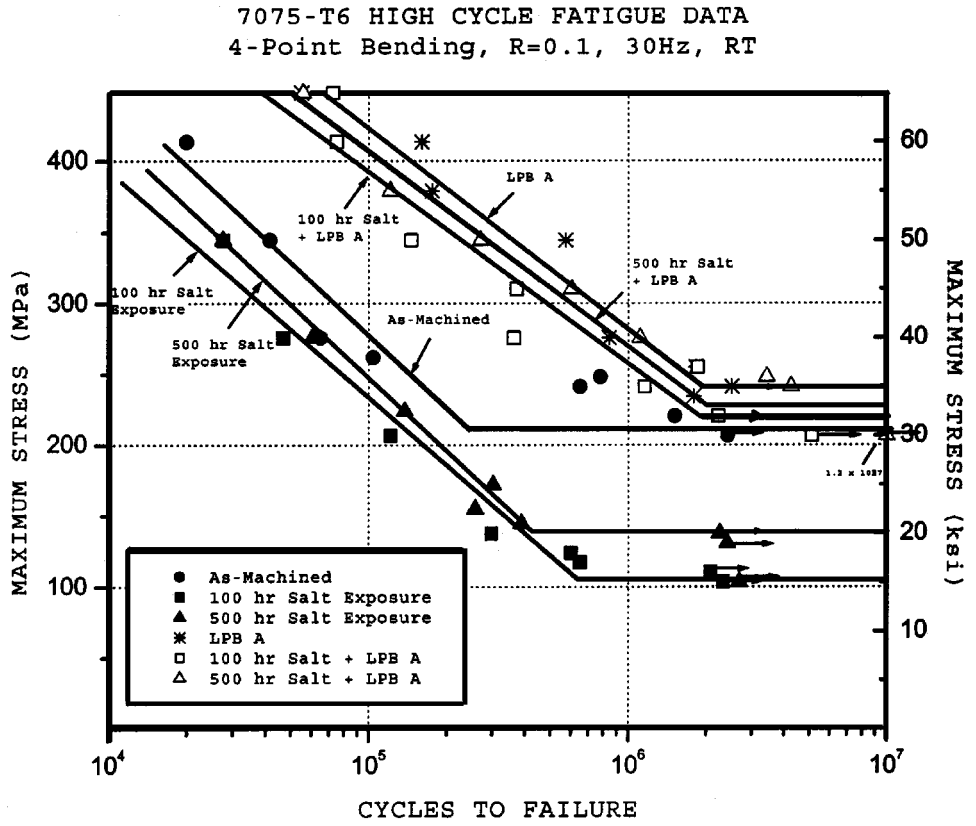

Fig. 6 HCF results for salt fog corroded 7075-T6

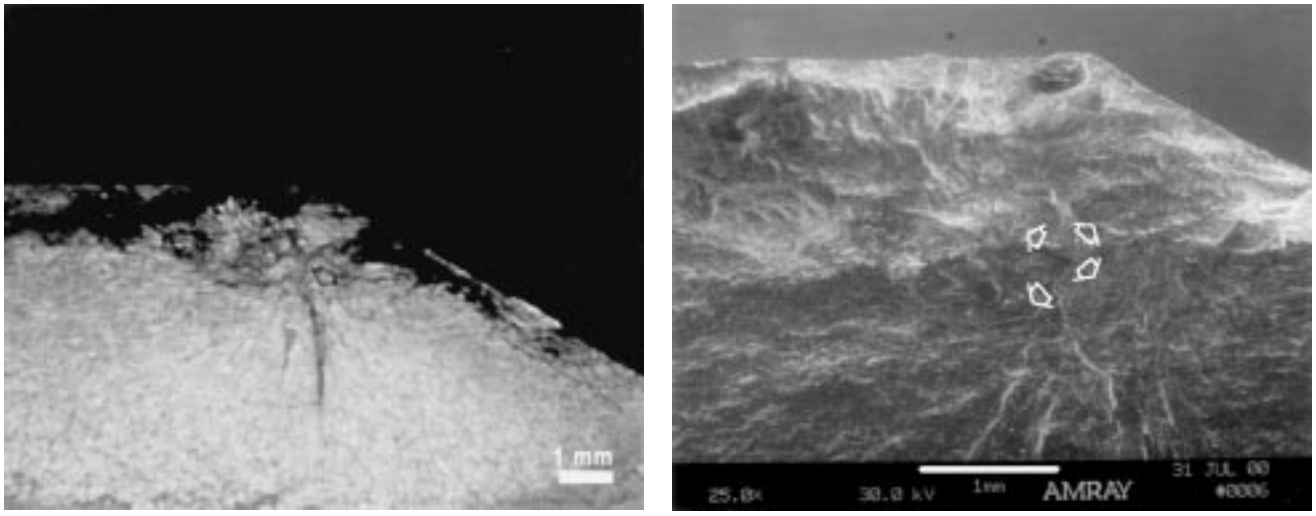

(**a**) (**b**)

Fig. 7 Macro (**a**) and SEM (**b**) views of subsurface nucleation in machined + LPB 7075-T6

The typical macroscopic appearance of a 100 h exposure is shown in Fig. 5(a). Fatigue failures in the salt fog exposed specimens initiated exclusively from corrosion pits. Specimens tested at lower stresses generally exhibited origins from a single pit, while specimens tested at higher stress levels tended to have multiple nucleation sites from separate pits. Pit depths were generally in the range of 0.10 to 0.13 mm (0.004 to 0.005 in.), although a few as deep as 0.25 mm (0.010 in.) were observed. Figure 5(b) shows an SEM micrograph of the same corrosion pit shown in Fig. 5(a).

The effect of LPB after machining (no corrosion) was to drive the fatigue origin subsurface by as much as 1 to 1.3 mm (0.04 to 0.05 in.). This is evidently beneath the compressive layer produced by LPB. Figure 7(a) shows the macroscopic appearance

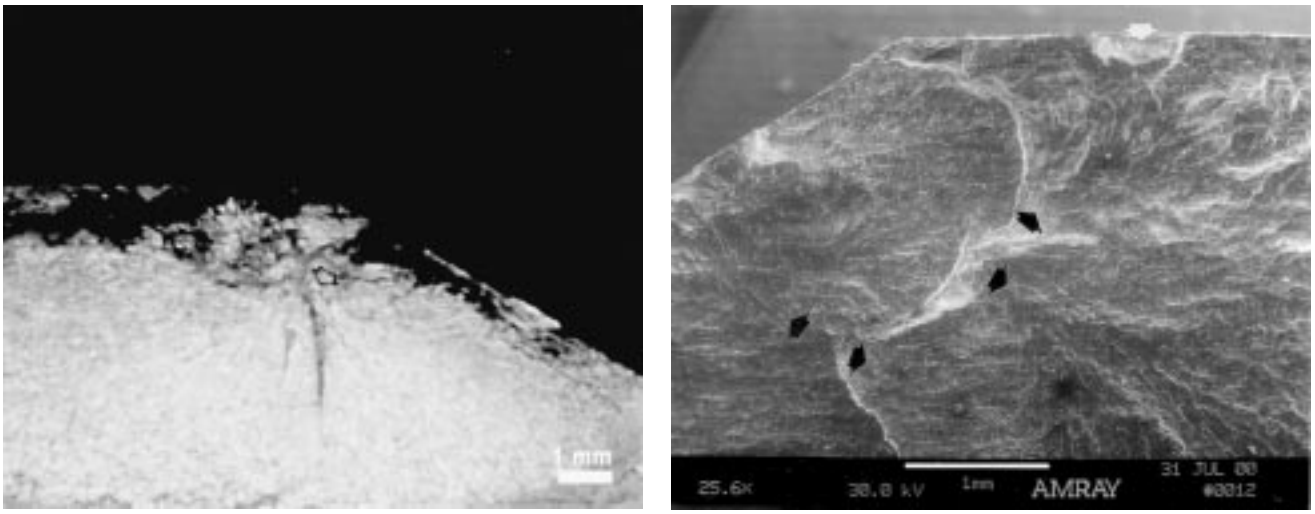

(**a**) (**b**)

Fig. 8 Macro (**a**) and SEM (**b**) and views of subsurface nucleation in 100 h salt fog + LPB 7075-T6

of the subsurface origin indicated by the arrow. An SEM micrograph in Fig. 7(b) shows the same origin at higher magnification. Arrows in Fig. 7(b) indicate the fatigue crack growth emanating in different directions from the subsurface origin.

The LPB treatment after salt fog exposure restored the fatigue strength too greater than as-machined levels. The strength restoration after LPB was the same for both the 100 and 500 h exposed conditions. Even after LPB processing, the corroded surface with pits was still very much in evidence, although the surface finish was substantially improved. The effect of LPB on fatigue failures in the corroded specimens was to drive the fatigue origin subsurface by 1 to 1.3 mm (0.04 to 0.05 in.) in the same manner as for the LPB processing of as-machined, noncorroded specimens. Figure 8(a) shows the macroscopic aspect of a subsurface origin (arrow) after 100 h salt fog exposure + LPB. The SEM micrograph (Fig. 8b) shows the same origin area. Here, with local crack growth directions indicated by black arrows, it can be seen that there are actually two subsurface origins. Moreover, the nearby surface pit indicated by the white arrow was rendered innocuous by the highly compressive stress produced by LPB and did not serve as a fatigue initiation site.

Conclusions

Low plasticity burnishing has been applied successfully to induce a layer of residual compression reaching the material yield strength beneath the surface and extending to a depth in excess of 1 mm (0.040 in.) in the aluminum alloy 7075-T6. Both the magnitude and depth of compression achieved exceed that produced by conventional shot peening.

Salt fog exposures of 100 and 500 h produced corrosion pits on the order of 0.13 mm (0.005 in.) with some extending to 0.25 mm (0.010 in.). As has been widely reported previously, fatigue cracks initiating from the salt pits reduced the 2×10^6 fatigue strength to half its initial value.

The LPB applied over the corroded surface, *without removing either the corrosion product or the pitted alloy layer*, resulted in full restoration of the fatigue strength at 2×10^6 cycles for either exposure. The surface finish was markedly improved. Fatigue crack nucleation from corrosion pits was eliminated. Failure after LPB processing occurred from subsurface nucleation sites in all cases. The fatigue life, at any stress examined above the endurance limit, was improved nominally by an order of magnitude.

Fatigue life improvement from LPB processing is attributed to the introduction of a layer of compressive residual stress of sufficient depth and magnitude to effectively close cracks emanating from corrosion pits shallower than the layer of compression, rendering them innocuous and altering the mode of fatigue crack nucleation. The compressive layer then retards the growth of fatigue cracks, which eventually nucleate, producing an order of magnitude life increase at stresses above the endurance limit.

Low plasticity burnishing has been demonstrated to restore the fatigue performance of severely salt fog corroded aluminum alloy 7075-T6. The ease of implementation in standard CNC machine centers offers the possibility of employing LPB as a low-cost effective means of mitigating corrosion fatigue failures in aluminum structural aircraft components.

References

1. V.S. Agarawala: *11th Annual AeroMat Conf.*, Bellevue, WA, June 26–29, 2000.
2. *ASM Handbook*, vol. 19, *Fatigue and Fracture*, S.R. Lampman, ed., American Society for Metals, Metals Park, OH, 1996.
3. N.E. Dowling: *Mechanical Behavior of Materials*, Prentice-Hall, Englewood Cliffs, NJ, 1993.
4. A.H. Clauer: in *Surface Performance of Titanium*, J.K. Gregory, H.J. Rack, and D. Eylon, eds., TMS, Warrendale, PA, 1996.
5. P.R. Smith, M.J. Shepard, P.S. Prevey, and A. Clauer: *Proc. 5th Nat. Turbine Engine HCF Conf.*, 2000.
6. P.S. Prevéy, J. Telesman, T. Gabb, and P. Kantzos: *Proc. 5th Natl. Turbine Engine HCF Conf.*, AFRL, WPAFB, Chandler, AZ, 2000.
7. P.S. Prevéy and M.J. Shepard: *11th AeroMat Conf.*, Bellevue, WA, June 26–29, 2000.

8. K.K. Sankaran, R. Perez, and K.V. Jata: *Advanced Materials Processing*, ASM International, Materials Park, OH, 2000, pp. 53-54.
9. D. Lombardo and P. Bailey: *6th Int. Conf. on Shot Peening*, J. Champaign, ed., AFRL, WPAFB, Chandler, AZ, 1996, pp. 493-504.
10. P. Prevéy: *Residual Stress in Design, Process & Material Selection*, American Society for Metals, Metals Park, OH.
11. U.S. Patent 5,826,453, Oct. 1998, other patents pending.
12. W. Zinn and B. Scholtes: *J. Mater. Eng. Performance*, 1999, vol. 8 (2), pp. 145-51.
13. I. Altenberger *et al.: Mater. Sci. Eng.*, 1999, vol. A264, pp. 1-16.
14. A. Drechsler, T. Dörr, and L. Wagner: *Mater. Sci. Eng.*, 1998, vol. A243, pp. 217-20.
15. P.S. Prevéy: *Metals Handbook*, American Society for Metals, Metals Park, OH, 1986.
16. *Residual Stress Measurement by XRD*, SAE J784a, M.E. Hilley, ed., SAE, Warrendale, PA, 1971.
17. Noyan and Cohen: *Residual Stress Measurement by Diffraction & Interpretation*, Springer-Verlag, New York, NY, 1987.
18. P. Prevey and W.P. Koster: *Fatigue at Elevated Temperatures*, ASTM STP561, ASTM, Philadelphia, PA, 1972.